# Heat conduction in one-dimensional aperiodic quantum Ising chains

Wenjuan Li[1] and Peiqing Tong[1,2,*]
[1]*Department of Physics and Institute of Theoretical Physics, Nanjing Normal University, Nanjing 210046, People's Republic of China*
[2]*Jiangsu Key Laboratory for Numerical Simulation of Large Scale Complex Systems, Nanjing Normal University, Nanjing 210046, People's Republic of China*
(Received 29 June 2010; revised manuscript received 22 October 2010; published 23 March 2011)

The heat conductivity of nonperiodic quantum Ising chains whose ends are connected with heat baths at different temperatures are studied numerically by solving the Lindblad master equation. The chains are subjected to a uniform transverse field $h$, while the exchange coupling $J_m$ between the nearest-neighbor spins takes the two values $J_A$ and $J_B$ arranged in Fibonacci, generalized Fibonacci, Thue-Morse, and period-doubling sequences. We calculate the energy-density profile and energy current of the resulting nonequilibrium steady states to study the heat-conducting behavior of finite but large systems. Although these nonperiodic quantum Ising chains are integrable, it is clearly found that energy gradients exist in all chains and the energy currents appear to scale as the system size $\langle Q\rangle \sim N^{\alpha}$. By increasing the ratio of couplings, the exponent $\alpha$ can be modulated from $\alpha > -1$ to $\alpha < -1$ corresponding to the nontrivial transition from the abnormal heat transport to the heat insulator. The influences of the temperature gradient and the magnetic field to heat conduction have also been discussed.

DOI: 10.1103/PhysRevE.83.031128 PACS number(s): 05.60.Gg, 05.30.−d, 61.44.Br, 05.70.Ln

## I. INTRODUCTION

Fourier's law, $\langle Q\rangle = -\kappa\nabla T$ stating that the heat flux per volume is proportional to the temperature gradient, was introduced as an empirical law in 1807. Many efforts have been focused on the issue of heat transport in the context of classical dynamic systems [1–8] (see, [1,2] for a review) and quantum dynamic systems [9–21], the origin of Fourier's law is still an open problem. In classical systems, an important issue is to determine the dependence of the heat current $\langle Q\rangle$ on the system size $N$. It is well known that heat transport scales as $\langle Q\rangle \sim N^0$ in integrable systems such as uniform or periodic chains, while one is expected as $\langle Q\rangle \sim N^{-1}$ according to Fourier's law [3]. Recently, a large number of studies have addressed that heat conductivity is abnormal with $\langle Q\rangle \sim N^{\alpha}$ in many one-dimensional systems, and the exponent $\alpha$ differs from model to model [4–8]. For example, it has been shown that the exponent $\alpha = -\frac{1}{2}$ in the case of a random harmonic chain [7]. It is also found that $-\frac{1}{2} < \alpha < 0$ shows up in some nonlinear aperiodic models [8].

Although many works have been devoted to investigating heat conduction in classical systems, much less is known about the properties of the thermal conductivity in quantum systems. For the quantum case, the extensively investigated systems are the spin chains [10–20] and the harmonic chains [21]. One main approach for the study of quantum thermal transport is the Green-Kubo formula, which is derived on the basis of linear response theory. Within this method, the thermal Drude weight has been calculated numerically in Refs. [10–13]. However, linear response theory only deals with a system near the equilibrium state. Furthermore, the validity of the Green-Kubo formula for thermal conduction is still questionable [22]. Another method to investigate the transport behavior of a quantum system is based on the quantum master equation (QME) [13–19]. One can use the direct numerical solution [13–17] or Monte Carlo wave-function approach [18,19] to find the stationary states of QME. For quantum integrable systems, it has been found that the transport behavior is ballistic and that the heat conductivity diverges in the thermodynamic limit $N \to \infty$ [11,15]. However, normal heat transport was observed for a small integrable spin chain [14]. By solving the QME for ten spin systems, Yan *et al.* found evidence of nonballistic heat conduction in an integrable random-exchange Ising chain [16]. Also diffusive heat transport has been found in an integrable spin chain with $N = 16$ by using the Monte Carlo wave-function technique [18].

However, all the investigations were generally focused on *small* system sizes due to the limitations of computer memory. Recently, Prosen proposed a new method to solve the Lindblad master equation of a general quadratic system with larger sizes $N$, ranging from 30 to 60. He found that heat transport scales as $\langle Q\rangle \sim N^0$ in a homogeneous transverse Ising chain and the currents decrease exponentially as $\langle Q\rangle \sim \exp(\alpha N)$ with $\alpha < 0$, which corresponds to the heat insulator, in a disordered Ising chain [17].

On the other hand, since the experimental discovery of quasicrystals [23] and the experimental work on Fibonacci superlattices [24], much attention has been focused on studies of one-dimensional nonperiodic systems [8,25–30]. Despite the absence of translational invariance in these structures, they show a long-range order. Such systems can be regarded as intermediate between uniform and random systems. It has been found that the electronic energy spectra of nonperiodic systems are singular continuous and the wave functions are critical, i.e., neither localized nor extended [25]. The phonon spectra of nonperiodic lattices are also shown to be Cantor-like, and they possess characteristics of both periodic and random systems [26]. Moreover, heat-transport properties of one-dimensional classical nonperiodic systems have been investigated [8,27].

Therefore, how the nonperiodicity affects the quantum thermal transport is an interesting problem. In this paper, we shall study the heat conduction in the nonperiodic quantum Ising chains. The rest of the paper is organized as follows. In Sec. II, we introduce the model. The method of solving the Lindblad master equation and the definitions for the energy

*Corresponding author: pqtong@njnu.edu.cn

 

density operator and the local energy current operator are given in Sec. III. Section IV contains our numerical results and the discussions of the transport properties of nonperiodic Ising chains. Finally, Sec. V is devoted to the summary and discussion.

## II. MODEL

To investigate the problem of nonperiodic quantum heat transport we choose to deal with one-dimensional finite open Ising chains whose two end spins are connected to heat baths with different temperatures. The total Hamiltonian is given by

$$H = H_S + H_B + H_I, \tag{1}$$

$$H_S = \sum_{m=1}^{N-1} J_m \sigma_m^x \sigma_{m+1}^x + \sum_{m=1}^{N} h\sigma_m^z, \tag{2}$$

where $H_S$, $H_B$, $H_I$ denote the Hamiltonian of the system, the baths' Hamiltonian, and the interaction between the system and the baths, respectively. We require the coupling between the system and the bath to be weak. In addition, $N$ is the number of spins, $\sigma_m^x$, $\sigma_m^z$ are the Pauli matrices for $m$th spin, $h$ is the uniform strength of the magnetic field, and $J_m$ is the nearest-neighbor coupling.

The special case of $J_m = J$ defines the uniform spin chain. For the random spin chain, $J_m$ is chosen as random uncorrelated variables. In our study, $J_m$ takes the two values $J_A$ and $J_B = J_A/\lambda$ according to the nonperiodic sequences. The most frequently studied nonperiodic sequence is the Fibonacci sequence, which is generated from a seed (e.g., $J_A$) by the following rule:

$$\begin{cases} J_A \to J_A J_B \\ J_B \to J_A \end{cases}. \tag{3}$$

The infinite Fibonacci sequence is given by

$$J_A J_B J_A J_A J_B J_A J_B J_A J_A J_B J_A J_A J_B \ldots .$$

Other well-studied nonperiodic systems are the generalized Fibonacci (GF), Thue-Morse (TM), and period-doubling (PD) lattices. They are built recursively from a seed (e.g., $J_A$) by the following rules:

$$\mathrm{GF}: \begin{cases} J_A \to J_A^m J_B^n \\ J_B \to J_A \end{cases},$$

$$\mathrm{TM}: \begin{cases} J_A \to J_A J_B \\ J_B \to J_B J_A \end{cases},$$

$$\mathrm{PD}: \begin{cases} J_A \to J_A J_B \\ J_B \to J_A J_A \end{cases},$$

respectively, where $m$,$n$ are positive integers and $J_A^m$ represents a string of $m$ $J_A$'s.

For the quantum integrable system the nearest-neighbor level spacing distribution $P(s)$ is a Poissonian distribution $P_P(s) = \exp(-s)$. In contrast, in the quantum chaotic system, $P(s)$ is typically the Wigner distribution $P_W(s) = (\pi s/2)\exp(-\pi s^2/4)$. After unfolding the energy spectra [31], we numerically calculate the $P(s)$ of the Hamiltonian (2)

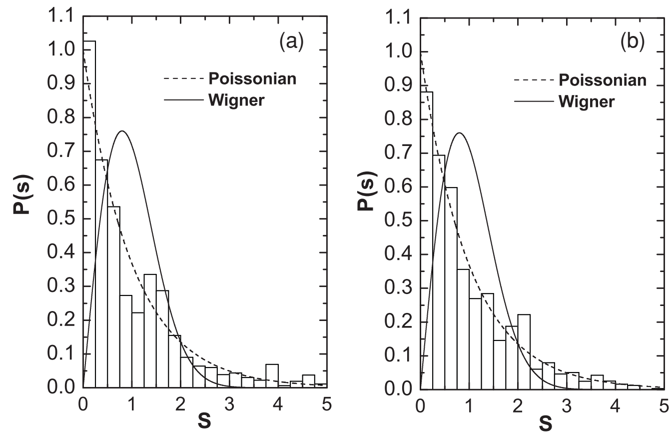


FIG. 1. Nearest-neighbor level spacing $P(s)$ for two typical cases. (a) Fibonacci Ising chain and (b) GF Ising chain with $m = 1$, $n = 4$, respectively. The Poisson distribution curve (dashed line) and the Wigner distribution curve (full line) are also shown. Here, $N = 10$, $h = 1.0$, $J_A = 1.5$, $\lambda = 1.5$.

and find that the nonperiodic Ising chains are integrable. Moreover, we find that the distribution $P(s)$ is independent of the parameters of $J_A$ and $\lambda$. Figure 1 shows the numerical results of $P(s)$ for the two typical examples: Fibonacci Ising chain and GF Ising chain with $m = 1$, $n = 4$. It is clear to see that the distributions $P(s)$ are close to the Poissonian distribution.

## III. LINDBLAD MASTER EQUATION AND ITS SOLUTION

Under the Born-Markovian approximation, the quantum Liouville equation of system (1) can be written in the Lindblad form [9,17] (we set $\hbar = 1$)

$$\frac{d\rho_s}{dt} = \hat{\mathcal{L}}\rho_s \equiv -i[H_S,\rho_s] + \sum_{\mu=1}^{4}(2L_\mu \rho_s L_\mu^\dagger - \{L_\mu^\dagger L_\mu,\rho_s\}), \tag{4}$$

where $[\ldots]$ and $\{\ldots\}$ denote the commutator and the anticommutator, while

$$\begin{aligned} L_1 &= \tfrac{1}{2}\sqrt{\Gamma_1^L}\sigma_1^-, \quad L_3 = \tfrac{1}{2}\sqrt{\Gamma_1^R}\sigma_N^-, \\ L_2 &= \tfrac{1}{2}\sqrt{\Gamma_2^L}\sigma_1^+, \quad L_4 = \tfrac{1}{2}\sqrt{\Gamma_2^R}\sigma_N^+. \end{aligned} \tag{5}$$

Here $L_\mu$ are operators representing couplings to different baths, and $\sigma_m^\pm = \sigma_m^x \pm i\sigma_m^y$. $\Gamma_{1,2}^L$ and $\Gamma_{1,2}^R$ denote the positive coupling constants related to bath temperatures. The temperatures of the two heat baths, $T_L$ and $T_R$, are embodied in the forms of $\Gamma_2^L/\Gamma_1^L = \exp(-2h_1/T_L)$ and $\Gamma_2^R/\Gamma_1^R = \exp(-2h_N/T_R)$. In our numerical calculation, we take bath couplings $\Gamma_1^L = \Gamma_1^R = 1.0$.

By using the Jordan-Wigner transformation, $\sigma_m^x = (-i)^{m-1}\prod_{j=1}^{2m-1}\omega_j$ and $\sigma_m^z = -i\omega_{2m-1}\omega_{2m}$, where $\omega_j$, $j = 1,2,\ldots,2N$, are Majorana operators with $\{\omega_j,\omega_k\} = 2\delta_{j,k}$, the Hamiltonian (2) can be written in terms of Majorana fermions as

$$H_S = -i\sum_{m=1}^{N-1} J_m \omega_{2m}\omega_{2m+1} - i\sum_{m=1}^{N} h\omega_{2m-1}\omega_{2m}. \tag{6}$$

To solve Eq. (4), Prosen [17] proposed the Fock space $\kappa$, which is a $4^N$-dimensional space of operators with a canonical basis $|P_{\underline{\alpha}}\rangle = P_{\alpha_1,\alpha_2,\ldots,\alpha_{2N}}|0\rangle \equiv \omega_1^{\alpha_1}\omega_2^{\alpha_2}\ldots\omega_{2N}^{\alpha_{2N}}|0\rangle$, $\alpha_j \in \{0,1\}$, and defined the annihilation operator $\hat{c}_j$ and the creation operator $\hat{c}_j^\dagger$ in terms of $\hat{c}_j|P_{\underline{\alpha}}\rangle = \delta_{\alpha_j,1}|\omega_j P_{\underline{\alpha}}\rangle$ and $\hat{c}_j^\dagger|P_{\underline{\alpha}}\rangle = \delta_{\alpha_j,0}|\omega_j P_{\underline{\alpha}}\rangle$, respectively. Here $\hat{c}_j$ and $\hat{c}_j^\dagger$ satisfy the canonical anticommutation relations $\{\hat{c}_j,\hat{c}_k\} = 0$, $\{\hat{c}_j,\hat{c}_k^\dagger\} = \delta_{jk}$, $j,k = 1,2,\ldots,2N$. Introducing the Hermitian Majorana operators $\hat{a}_{2j-1} = \frac{1}{\sqrt{2}}(\hat{c}_j + \hat{c}_j^\dagger)$, $\hat{a}_{2j} = \frac{i}{\sqrt{2}}(\hat{c}_j - \hat{c}_j^\dagger)$ with $\hat{a}_r = \hat{a}_r^\dagger$, $\{\hat{a}_r,\hat{a}_s\} = \delta_{r,s}$, $r = 1,2,\ldots,4N$, the Lindblad equation (4) can be written as

$$\hat{\mathcal{L}} = \underline{\hat{a}} \cdot \mathbf{A}\underline{\hat{a}} + \mathrm{const}\,\mathbb{1}. \tag{7}$$

Here $\underline{\hat{a}} \equiv (\hat{a}_1,\hat{a}_2,\ldots,\hat{a}_{4N})^T$. $\mathbf{A}$ is a $4N \times 4N$ dimensional and antisymmetric complex matrix whose eigenvalues are complex and come in pairs $\beta_1, -\beta_1,\ldots,\beta_{2N}, -\beta_{2N}$. The corresponding eigenvectors are the solutions of equations $\mathbf{A}\underline{v}_{2j-1} = \beta_j\underline{v}_{2j-1}$ and $\mathbf{A}\underline{v}_{2j} = -\beta_j\underline{v}_{2j}$ $(j = 1,2,\ldots,2N)$. By introducing the linear maps $\hat{b}_j = \underline{v}_{2j-1}\cdot\underline{\hat{a}}$ and $\hat{b}_j' = \underline{v}_{2j}\cdot\underline{\hat{a}}$, $\{\hat{b}_j,\hat{b}_k\} = \{\hat{b}_j',\hat{b}_k'\} = 0$, $\{\hat{b}_j,\hat{b}_k'\} = \delta_{j,k}$, the Liouvillean (7) can be written into a very convenient normal form $\hat{\mathcal{L}} = -2\sum_{j=1}^{2N}\beta_j\hat{b}_j'\hat{b}_j$. The complete set of $4^N$ eigenvalues of $\hat{\mathcal{L}}$ are obtained by all the possible binary linear combinations $-2\sum_j n_j\beta_j$, where $n_j \in \{0,1\}$ are eigenvalues of $2N$ mutually commuting non-Hermitian number operators $\hat{b}_j'\hat{b}_j$. Let the nonequilibrium steady state $|\mathrm{NESS}\rangle$ be the element of Fock space $\kappa$ corresponding to the zero eigenvalue of the Liouvillean (7), i.e., $n_j = 0$.

Prosen [17] has proven that expectation values of the quadratic operators in $\rho_{\mathrm{NESS}}$ which is the stationary solution of the Lindblad equation (4) can be explicitly computed as

$$\begin{aligned}\langle\omega_j\omega_k\rangle_{\mathrm{NESS}} &= tr(\omega_j\omega_k\rho_{\mathrm{NESS}})\\ &= \delta_{j,k} + \langle\mathbb{1}|\hat{c}_j\hat{c}_k|\mathrm{NESS}\rangle\\ &= \delta_{j,k} + \frac{1}{2}\sum_{m=1}^{2N}(v_{2m,2j-1}v_{2m-1,2k-1} - v_{2m,2j}v_{2m-1,2k}\\ &\quad - i\,v_{2m,2j}v_{2m-1,2k-1} - i\,v_{2m,2j-1}v_{2m-1,2k}).\end{aligned} \tag{8}$$

Here $v_{r,s}$ is the component $s$ $(s = 1,2,\ldots,4N)$ of the $r$th right eigenvector $\underline{v_r}$ $(r = 1,2,\ldots,4N)$ of the matrix $\mathbf{A}$ (7).

In our system, $\mathbf{A}$ is written as

$$\mathbf{A} = \begin{pmatrix} \mathbf{B}_L - h\mathbf{R} & \mathbf{R}_1 & 0 & \ldots & 0\\ -\mathbf{R}_1^T & -h\mathbf{R} & \mathbf{R}_2 & \ddots & 0\\ 0 & -\mathbf{R}_2^T & -h\mathbf{R} & & \vdots\\ \vdots & \ddots & & \ddots & \mathbf{R}_{N-1}\\ 0 & 0 & \ldots & -\mathbf{R}_{N-1}^T & \mathbf{B}_R - h\mathbf{R}\end{pmatrix}. \tag{9}$$

Here,

$$\mathbf{R} = \begin{pmatrix} 0 & 0 & 1 & 0\\ 0 & 0 & 0 & 1\\ -1 & 0 & 0 & 0\\ 0 & -1 & 0 & 0\end{pmatrix}, \tag{10}$$

$$\mathbf{R}_m = \begin{pmatrix} 0 & 0 & 0 & 0\\ 0 & 0 & 0 & 0\\ -J_m & 0 & 0 & 0\\ 0 & -J_m & 0 & 0\end{pmatrix}, \tag{11}$$

$$\mathbf{B}_L = \begin{pmatrix} 0 & \frac{i}{2}\Gamma_+^L & -\frac{i}{2}\Gamma_-^L & \frac{1}{2}\Gamma_-^L\\ -\frac{i}{2}\Gamma_+^L & 0 & \frac{1}{2}\Gamma_-^L & \frac{i}{2}\Gamma_-^L\\ \frac{i}{2}\Gamma_-^L & -\frac{1}{2}\Gamma_-^L & 0 & \frac{i}{2}\Gamma_+^L\\ -\frac{1}{2}\Gamma_-^L & -\frac{i}{2}\Gamma_-^L & -\frac{i}{2}\Gamma_+^L & 0\end{pmatrix}, \tag{12}$$

and

$$\mathbf{B}_R = \begin{pmatrix} 0 & \frac{i}{2}\Gamma_+^R & -\frac{i}{2}\Gamma_-^R & \frac{1}{2}\Gamma_-^R\\ -\frac{i}{2}\Gamma_+^R & 0 & \frac{1}{2}\Gamma_-^R & \frac{i}{2}\Gamma_-^R\\ \frac{i}{2}\Gamma_-^R & -\frac{1}{2}\Gamma_-^R & 0 & \frac{i}{2}\Gamma_+^R\\ -\frac{1}{2}\Gamma_-^R & -\frac{i}{2}\Gamma_-^R & -\frac{i}{2}\Gamma_+^R & 0\end{pmatrix}, \tag{13}$$

respectively, where $\Gamma_\pm^L = \Gamma_2^L \pm \Gamma_1^L$ and $\Gamma_\pm^R = \Gamma_2^R \pm \Gamma_1^R$.

Based on the Majorana operators [17], the local energy-density operator can be explicitly defined as

$$\begin{aligned} H_m = -i\,J_m\omega_{2m}\omega_{2m+1} - \frac{i h_m}{2}\omega_{2m-1}\omega_{2m}\\ - \frac{i h_{m+1}}{2}\omega_{2m+1}\omega_{2m+2},\end{aligned} \tag{14}$$

and the local energy current operator can be derived from the equation of continuity

$$\begin{aligned} Q_m &\equiv [H_m,H_{m+1}]\\ &= 2i(-J_m h_{m+1}\omega_{2m}\omega_{2m+2} - h_{m+1}J_{m+1}\omega_{2m+1}\omega_{2m+3}).\end{aligned} \tag{15}$$

Note that the above two observable operators $H_m$ and $Q_m$ are written in the quadratic form. Thus it is easy to calculate their expectation values in $\rho_{\mathrm{NESS}}$.

## IV. NUMERICAL RESULTS

In the following, we first investigate the heat conduction of the Fibonacci Ising chain. Due to the nonuniformity of the nonperiodic chain, the numerical results need to be averaged as done in the random case. In our numerical calculation, we generate a very long but finite Fibonacci sequence of size $L$ $(L \gg N)$ according to the rule (3). For $N$-spin chain, we select $N-1$ consecutive couplings, while the starting position is on a random position of the Fibonacci sequence. Then we obtain the expectation values of operators $H_m$ and $Q_m$ in $\rho_{\mathrm{NESS}}$ for the spin chain with the above-chosen couplings. Finally, we perform the average over 2000 realizations. In short, we use $\langle H_m\rangle$ and $\langle Q_m\rangle$ to denote the average energy density and the average energy current. Throughout the paper, the temperatures of baths are set as $T_R = T_0(1+\delta T)$, $T_L = T_0(1-\delta T)$.

Figure 2(a) shows the energy profiles of Fibonacci Ising chains with $\lambda = 1.5$ but with different sizes $N$, ranging from $N = 20$ to $N = 60$. For the quantum system, Fourier's law intuitively translates into $\langle Q\rangle \sim \nabla\langle H_m\rangle$, where the local energy plays the role of the temperature. We observe that in the

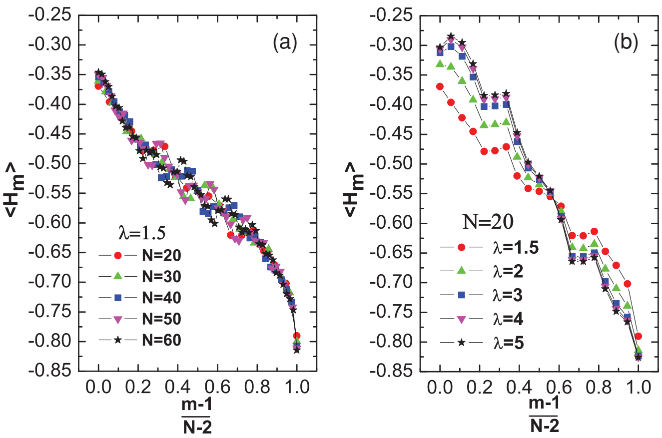


FIG. 2. (Color online) Scaled energy profiles of Fibonacci Ising chains for different $N$ and $\lambda$, respectively. (a) $\lambda = 1.5$, $N = 20$ (red dot), $N = 30$ (green upward-pointing triangle), $N = 40$ (blue square), $N = 50$ (magenta downward-pointing triangle), $N = 60$ (black star); (b) $N = 20$, $\lambda = 1.5$ (red dot), $\lambda = 2$ (green upward-pointing triangle), $\lambda = 3$ (blue square), $\lambda = 4$ (magenta downward-pointing triangle), $\lambda = 5$ (black star). Here $h = 1.5$, $J_A = 1.5$, $T_0 = 5$, $\delta T = 0.5$.

bulk of chains energy gradients are formed for any system size. In Fig. 2(b), we show the energy profile with fixed system size $N = 20$, while the ratio of couplings range from $\lambda = 1.5$ to $\lambda = 5$. It is also clear to see that energy gradients are built in all chains for different ratios of couplings. Contrary to the ballistic transport in the uniform quantum Ising chain [16,17], the dissipative transport behavior can be observed in the Fibonacci Ising chains with different system sizes or with different ratios of the couplings.

We now turn to investigate the energy current of the Fibonacci Ising chain. The local energy current $\langle Q_m \rangle$ in $\rho_{\mathrm{NESS}}$ does not depend on the special chain site, i.e., $\langle Q_m \rangle = \langle Q \rangle$. In Fig. 3 , we present the energy currents $\langle Q \rangle$ versus $N$ for different values of the ratio $\lambda$. It is clear to find that energy currents all behave as $\langle Q \rangle \sim N^{\alpha}$ in the asymptotic regime $N \gg 1$, where $\alpha$ depends on the ratio of couplings $\lambda$. The inset of Fig. 3 shows the dependence of $\alpha$ on the ratio of $\lambda$. When $\lambda \to 1$, it is found that the exponent $\alpha \to 0$ and the energy gradient vanish, which could be interpreted as the ballistic transport. When $\lambda \to \lambda_c \approx 3.0$, $\alpha$ is found to be $-1$, which corresponds to the normal heat transport. For the case of $1 < \lambda < \lambda_c$, the exponent $\alpha$ is $-1 < \alpha < 0$ implying an anomalous heat conduction. And for the case of $\lambda > \lambda_c$, $\alpha < -1$ results in the thermal insulator. Therefore, with increasing ratios $\lambda$, a nontrivial transition, which is from abnormal heat conduction to the thermal insulator heat transport, has been found in Fibonacci Ising chains. Moreover, one can conclude that transport behaviors of Fibonacci Ising chains are different from those of disordered Ising chains whose average currents decrease exponentially as $\langle Q \rangle \sim \exp(\alpha N)$ with $\alpha < 0$ [17].

In order to investigate the effect of the temperature gradient on transport properties, we also study the energy current of Fibonacci Ising chains in different temperatures of the heat baths. Figure 4(a) shows the numerical results of the energy current at the same temperature $T_0$, but with different

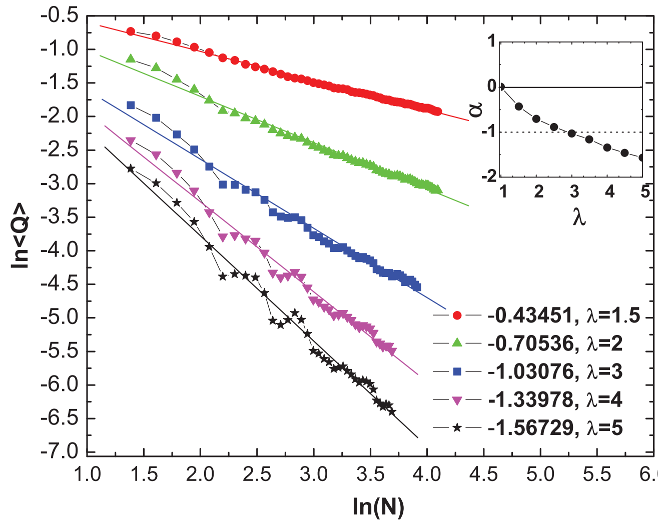


FIG. 3. (Color online) Energy current $\langle Q \rangle$ of Fibonacci Ising chains versus the chain length $N$ for different $\lambda$. Here $\lambda = 1.5$ (red dot), $\lambda = 2$ (green upward-pointing triangle), $\lambda = 3$ (blue square), $\lambda = 4$ (magenta downward-pointing triangle), $\lambda = 5$ (black star). The inset shows the dependence of $\alpha$ on the ratio of $\lambda$. The solid line represents ballistic transport, and the dotted line stands for the normal transport. Here, $h = 1.5$, $J_A = 1.5$, $T_0 = 5$, $\delta T = 0.5$.

$\delta T = 0.9, 0.5, 0.1$, respectively. Figure 4(b) shows the numerical data of the energy current at a fixed temperature gradient $\delta T = 0.5$, and $T_0 = 10, 5, 1$, respectively. Our numerical data indicate that transport properties, i.e., $\langle Q \rangle \sim N^{\alpha}$, are independent of external temperature and the temperature gradient. The results are in accordance with those of Prosen for a disordered Ising chain [17].

In addition, we study the heat conduction of other nonperiodic Ising chains. In Fig. 5, we show the energy currents of the GF, TM, and PD Ising chains, respectively. Generally, the nonperiodic chains can be classified into two classes depending on the "wandering exponent" $\beta$, where $\beta = \ln|\lambda_2| / \ln \lambda_1$ ($\lambda_1$, $\lambda_2$ are the leading and next-to-leading eigenvalues of the

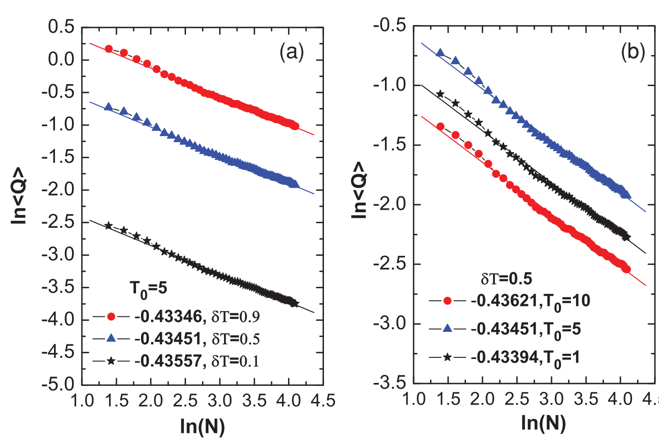


FIG. 4. (Color online) Energy current $\langle Q \rangle$ of Fibonacci Ising chains versus the chain length $N$ for different $\delta T$ and $T_0$, respectively. (a) $T_0 = 5$, $\delta T = 0.9$ (red dot), $\delta T = 0.5$ (blue triangle), $\delta T = 0.1$ (black star); (b) $\delta T = 0.5$, $T_0 = 10$ (red dot), $T_0 = 5$ (blue triangle), $T_0 = 1$ (black star). Here $h = 1.5$, $J_A = 1.5$, $\lambda = 1.5$.

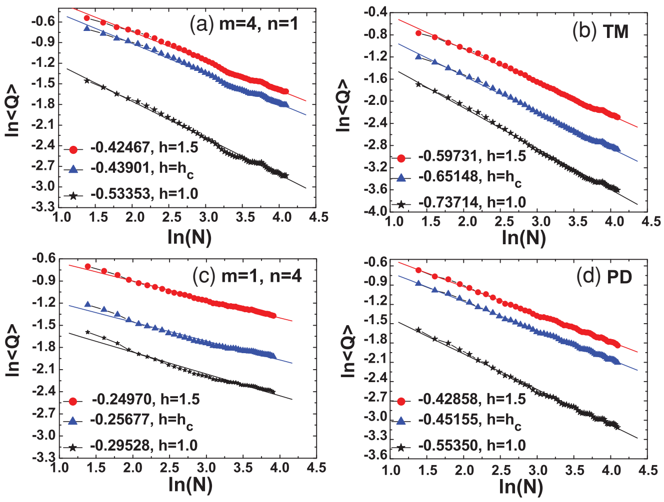


FIG. 5. (Color online) Energy current $\langle Q \rangle$ versus the chain length $N$ for four kinds of nonperiodic Ising chains. (a) GF ($m = 4, n = 1$), (b) TM, (c) GF ($m = 1$, $n = 4$), and (d) PD. Here, $J_A = 1.5$, $\lambda = 1.5$, $T_0 = 5$, $\delta T = 0.5$, and $h = 1.5 > h_c$ (red dot), $h =$ critical point (blue triangle), $h = 1.0 < h_c$ (black star).

substitute matrix) describes the fluctuations in the coupling. The Fibonacci chain, GF chains with $m \geqslant 1$, $n = 1$, and TM chain belong to the first class with $\beta < 0$. This class has the Pisot-Vijayaraghavan property that only one of the eigenvalues of the substitute matrix in absolute is larger than unity. In contrast, the GF chains with $m = 1$, $n > 1$, and PD chain belong to the second class with $\beta \geqslant 0$. This class is known to be non-Pisot [28,29]. From the studies of electronic energy spectra [25] and trace map [30] of these nonperiodic systems, one can conclude that either the electronic energy spectra or the trace map of the first class nonperiodic chains are different from that of the second class. However, our numerical results clearly indicate that the energy gradients exist in the two classes of nonperiodic chains, and the energy currents all scale as $\langle Q \rangle \sim N^{\alpha}$ with $\alpha$ depending on the values of $\lambda$. It is also interesting to remark that the exponents $\alpha$ are not universal values in the same class of nonperiodic chains.

For the quantum Ising chain, it is well known that the system has one zero-temperature quantum phase transition point (QPT) at $h_c^N = \prod_{m=1}^{N} J_m$ in the thermodynamic limit $N \to \infty$, where $N$ is the length of the chain [29]. The transition is from a ferromagnetic phase with long-range correlation in the $x$ direction to a paramagnetic phase. The QPTs of the nonperiodic chains belong to the universality class of a uniform quantum Ising chain and of a random quantum Ising chain for $\beta < 0$ and $\beta > 0$, respectively [29]. In Fig. 5, we also plot the energy current $\langle Q \rangle$ with $h < h_c$, $h = h_c$, and $h > h_c$, respectively. The numerical results show that energy currents with different values of $h$ hold the same characters $\langle Q \rangle \sim N^{\alpha}$ for all the nonperiodic Ising chains. Here $\alpha$ for $h > h_c$ is a little larger than that for $h < h_c$, and $\alpha$ for critical point is intermediate between the values of the two cases above. Moreover, the exponents $\alpha$ at the critical points depend on the structures of nonperiodic Ising chains. Even the QPTs of the two nonperiodic Ising chains belong to the same universality class, their exponents $\alpha$ at critical points are different from each other [see Fig. 5(a) and 5(b)]. It is due to the energy current $\langle Q \rangle$, which is an averaged value in $\rho_{\text{NESS}}$ containing excited states and thermal fluctuations.

## V. SUMMARY AND DISCUSSION

In summary, we perform a detailed analysis of heat conductivity in nonperiodic quantum Ising chains by solving the Lindblad master equation. The chains are connected to two heat baths with different temperatures and subjected to the uniform magnetic field $h$, while the exchange couplings $\{J_m\}$ between the nearest-neighbor spins are generated by the nonperiodic rules. Although these nonperiodic Ising chains are integrable, the energy gradients exist in all chains for any system size or any ratio of couplings, and the energy currents behave as $\langle Q \rangle \sim N^{\alpha}$, which is different from the transport behavior $\langle Q \rangle \sim \exp(\alpha N)$ in a random Ising chain and the ballistical heat transport $\langle Q \rangle \sim N^0$ in a homogeneous transverse Ising chain. We find that the heat transport in the nonperiodic Ising chain could be modulated from the abnormal heat transport ($\alpha > -1$) to the thermal insulating behavior ($\alpha < -1$) by increasing the ratio of couplings. Also the heat transport properties of $\langle Q \rangle \sim N^{\alpha}$ are independent of temperature gradient. Moreover, numerical evidence is provided such that the energy currents with different values of $h$ all behave as $\langle Q \rangle \sim N^{\alpha}$, but the exponent $\alpha$ is a function of the magnetic field $h$ and the ratio of couplings $\lambda$. In particular, the exponents $\alpha$ of nonperiodic Ising chains at critical points depend on the structures of spin chains.

## ACKNOWLEDGMENTS

We would like to thank Ye Xiong and Zhenjun Zhang for the valuable discussions. This project was supported by the National Natural Science Foundation of China (Grant No. 10974097), and by National Key Projects for Basic Research of China (Grant No. 2009CB929501).

[1] F. Bonetto, J. L. Lebowitz, and L. Rey-Bellet, *Fourier's Law: A Challenge to Theorists* (Imperial College Press, London, 2000).

[2] S. Lepri, R. Livi, and A. Politi, Phys. Rep. **377**, 1 (2003).

[3] G. Casati, J. Ford, F. Vivaldi, and W. M. Visscher, Phys. Rev. Lett. **52**, 1861 (1984); B. Hu, B. Li, and H. Zhao, Phys. Rev. E **57**, 2992 (1998).

[4] S. Lepri, R. Livi, and A. Politi, Phys. Rev. Lett. **78**, 1896 (1997).

[5] T. Prosen and D. K. Campbell, Phys. Rev. Lett. **84**, 2857 (2000); O. Narayan and S. Ramaswamy, *ibid.* **89**, 200601 (2002); T. Mai, A. Dhar, and O. Narayan, *ibid.* **98**, 184301 (2007).

[6] C. Giardiná, R. Livi, A. Politi, and M. Vassalli, Phys. Rev. Lett. **84**, 2144 (2000); O. V. Gendelman and A. V. Savin, *ibid.* **84**, 2381 (2000).

[7] A. Dhar, Phys. Rev. Lett. **86**, 5882 (2001).

[8] P. Tong, B. Li, and B. Hu, Phys. Rev. B **59**, 8639 (1999); Y. Zhang and H. Zhao, Phys. Rev. E **66**, 026106 (2002).

[9] H. -P. Breuer and F. Petruccione, *The Theory of Open Quantum Systems* (Oxford University Press, Oxford, 2002).
[10] M. Michel, J. Gemmer, and G. Mahler, Int. J. Mod. Phys. B **20**, 4855 (2006).
[11] X. Zotos, F. Naef, and P. Prelovsek, Phys. Rev. B **55**, 11029 (1997).
[12] F. Heidrich-Meisner, A. Honecker, D. C. Cabra, and W. Brenig, Phys. Rev. B **66**, 140406(R) (2002); **68**, 134436 (2003).
[13] K. Satio, Europhys. Lett. **61**, 34 (2003).
[14] M. Michel, M. Hartmann, J. Gemmer, and G. Mahler, Eur. Phys. J. B **34**, 325 (2003).
[15] K. Saito, S. Takesue, and S. Miyashita, Phys. Rev. E **54**, 2404 (1996).
[16] Y. Yan, C. Q. Wu, G. Casati, T. Prosen, and B. Li, Phys. Rev. B **77**, 172411 (2008).
[17] T. Prosen, New J. Phys. **10**, 043026 (2008).
[18] M. Michel, O. Hess, H. Wichterich, and J. Gemmer, Phys. Rev. B **77**, 104303 (2008).
[19] C. Mejia-Monasterio and H. Wichterich, Eur. Phys. J. Spec. Top. **151**, 113 (2007).
[20] C. Mejia-Monasterio, T. Prosen, and G. Casati, Europhys. Lett. **72**, 520 (2005).
[21] C. Gaul, and H. Büttner, Phys. Rev. E **76**, 011111 (2007); A. F. Neto, H. C. F. Lemos, and E. Pereira, *ibid*. **76**, 031116 (2007).
[22] J. Gemmer, R. Steinigeweg, and M. Michel, Phys. Rev. B **73**, 104302 (2006), and references therein.
[23] D. Shechtman, I. Blech, D. Gratias, and J. W. Cahn, Phys. Rev. Lett. **53**, 1951 (1984).
[24] R. Merlin, K. Bajema, R. Clarke, F. Y. Juang, and P. K. Bhattacharya, Phys. Rev. Lett. **55**, 1768 (1985).
[25] H. Hiramoto and M. Kohmoto, Int. J. Mod. Phys. **6**, 281 (1992); M. Kohmoto, L. P. Kadanoff, and C. Tang, Phys. Rev. Lett. **50**, 1870 (1983).
[26] J. P. Lu, T. Odagaki, and J. L. Birman, Phys. Rev. B **33**, 4809 (1986); S. Tamura and F. Nori, *ibid*. **40**, 9790 (1989).
[27] N. Nishiguchi, N. Takahashi, and T. Sakuma, J. Phys. Condens. Matter. **4**, 1465 (1992); E. Maciá, Phys. Rev. B **61**, 6645 (2000); M. Torikai and T. Odagaki, J. Phys. Condens. Matter. **14**, L503 (2002).
[28] See, for example, C. Godrèche and J. M. Luck, Phys. Rev. B **45**, 176 (1992), and references therein.
[29] J. M. Luck, J. Stat. Phys. **72**, 417 (1993).
[30] G. Gumbs and M. K. Ali, Phys. Rev. Lett. **60**, 1081 (1988).
[31] O. Bohigas, M. J. Giannoni, and C. Schmit, Phys. Rev. Lett. **52**, 1 (1984).